AD-A055 580 ARMY ELECTRONICS RESEARCH AND DEVELOPMENT COMMAND WS--ETC F/G 17/5
WATER VAPOR CONTINUUM ABSORPTION IN THE 3.5 MICROMETERS TO 4.0 --ETC(U)
MAR 78 K O WHITE, W R WATKINS, C W BRUCE

UNCLASSIFIED ERADCOM/ASL-TR-0004 NL

| OF |
AD
A055 580

END
DATE
FILMED
8-78
DDC

ASL - TR - 0004

WATER VAPOR CONTINUUM ABSORPTION IN THE 3.5μm TO 4.0μm REGION

MARCH 1978

By

Kenneth O. White, Wendell R. Watkins, and Charles W. Bruce

US ARMY ATMOSPHERIC SCIENCES LABORATORY
White Sands Missile Range, New Mexico 88002

Robert E. Meredith and Frederick G. Smith

SCIENCE APPLICATIONS, INC.
15 Research Drive
Ann Arbor, Michigan 48107

US Army Electronics Research and Development Command
Atmospheric Sciences Laboratory
White Sands Missile Range, N.M. 88002

NOTICES

Disclaimers

The findings in this report are not to be construed as an official Department of the Army position, unless so designated by other authorized documents.

The citation of trade names and names of manufacturers in this report is not to be construed as official Government indorsement or approval of commercial products or services referenced herein.

Disposition

Destroy this report when it is no longer needed. Do not return it to the originator.

(14) ERADCOM/ASL-TR-0004

SECURITY CLASSIFICATION OF THIS PAGE (When Data Entered)

REPORT DOCUMENTATION PAGE

READ INSTRUCTIONS BEFORE COMPLETING FORM

1. REPORT NUMBER: ASL-TR-0004

2. GOVT ACCESSION NO.

3. RECIPIENT'S CATALOG NUMBER

4. TITLE (and Subtitle): (6) WATER VAPOR CONTINUUM ABSORPTION IN THE ~~3.5μm TO 4.0μm REGION~~ 3.5 micrometers to 4.Ø micrometers Region.

5. TYPE OF REPORT & PERIOD COVERED: (7) R&D Technical Report.

6. PERFORMING ORG. REPORT NUMBER

7. AUTHOR(s): K. O. White, W. R. Watkins, and C. W. Bruce, ASL, ERADCOM; R. E. Meredith and F. G. Smith, Sci Appl., Inc.

8. CONTRACT OR GRANT NUMBER(s)

9. PERFORMING ORGANIZATION NAME AND ADDRESS: Atmospheric Sciences Laboratory, White Sands Missile Range, New Mexico 88002

10. PROGRAM ELEMENT, PROJECT, TASK AREA & WORK UNIT NUMBERS: (16) DA Task 1L161102B53A

11. CONTROLLING OFFICE NAME AND ADDRESS: US Army Electronics Research and Development Command, Adelphi, Maryland 20783

12. REPORT DATE: (11) March 1978

13. NUMBER OF PAGES: 35 (12) 35 p.

14. MONITORING AGENCY NAME & ADDRESS (if different from Controlling Office): (10) Kenneth O. /White, Wendell R. /Watkins, Charles W. /Bruce, Robert E. /Meredith, Frederick G. /Smith

15. SECURITY CLASS. (of this report): UNCLASSIFIED

15a. DECLASSIFICATION/DOWNGRADING SCHEDULE

16. DISTRIBUTION STATEMENT (of this Report)

Approved for public release; distribution unlimited.

17. DISTRIBUTION STATEMENT (of the abstract entered in Block 20, if different from Report)

18. SUPPLEMENTARY NOTES

19. KEY WORDS (Continue on reverse side if necessary and identify by block number)

Absorption	Lasers
Atmospheric optics	Spectroscopy
Infrared	Water vapor

MICRON

20. ABSTRACT (Continue on reverse side if necessary and identify by block number)

Measurements of water vapor continuum absorption in the 3.5(μm) to 4.0(μm) region are presented. The measurements were made with both long-path absorption cell and spectrophone systems. A deuterium fluoride grating tunable laser was the infrared source. Measurements were made at 23°C and 65°C with 14.3 torr and 65 torr of water vapor, respectively, buffered to 760 torr total pressure by an 80/20 mixture of N_2/O_2. Both natural water and a special sample of deuterium depleted water (one-fiftieth the normal concentration) were used. The

DD FORM 1 JAN 73 1473 EDITION OF 1 NOV 65 IS OBSOLETE

SECURITY CLASSIFICATION OF THIS PAGE (When Data Entered)

JTC

410 663

20. ABSTRACT (Cont)

independent measurements of water vapor continuum absorption using long-path cell and spectrophone systems with both natural and deuterium depleted water vapor all agree to within the experimental uncertainty (~25%). The 65°C results agree with previous measurements by other workers. The 23°C results indicate a continuum absorption at this temperature about a factor of 2 larger than expected based on the extrapolation scheme and high-temperature data ($\geq$65°C) of others. These results increase the accuracy of the data base used for modeling the atmospheric transmission effects on Army EO Systems.

SUMMARY

This report presents measurements of water vapor continuum absorption in the 3.5μm to 4.0μm region at 65°C and 23°C. The 23°C measurements are the first reported at a temperature below 65°C, to our knowledge. Measurements made at the higher temperature agree with those of Burch, et al. The most significant result of the present investigation is that the air-broadened water vapor continuum at 23°C is some 2 to 3 times greater than expected based on the high-temperature data and extrapolation procedure of Burch et al. This is significant not only because the greater absorption we measure has impact on practical applications, but also because it indicates at this time that the temperature dependence of the continuum at the lower temperature above and below ambient is in question.

The greater absorption at 23°C than expected from the Burch extrapolation also implies a wide bound of uncertainty in the room temperature values of C_s and C_f and for the ratio B* for air-broadened water vapor in this spectral region. This is a question which has great practical significance for electro-optical imaging systems' performance, since transmission as a function of range and humidity is sensitive to the magnitude of these parameters. In the absence of self- and air-broadened water vapor data required to determine C_f, C_s or even B*, it is not possible to identify the mechanism by which the water vapor (continuum) absorbs in this spectral region. Measurements on self- and foreign-broadened water vapor directed to answering this question are in progress in our laboratory and will be reported at a later date.

The results presented in this report will increase the accuracy of modeling results used for the performance prediction and evaluation of Army and DoD EO and HEL Systems.

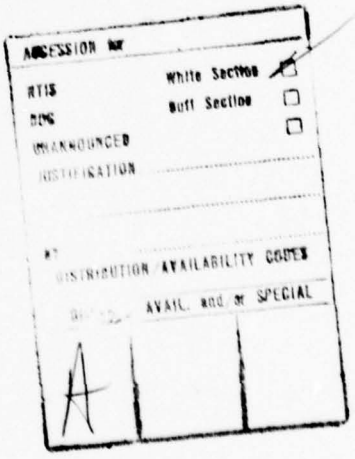

PREFACE

The authors gratefully acknowledge the help of Brian Z. Sojka in the data-taking portion of this work and Drs. Donald E. Snider and David G. Snyder for their critical reviews of the manuscript.

CONTENTS

INTRODUCTION

An accurate and detailed knowledge of atmospheric transmission in and near the infrared spectral windows is essential to the design, performance evaluation, and comparative testing of electro-optical (EO) systems. For example, atmospheric transmission is an important factor in the selection of optimum spectral bands for infrared imaging systems. The transmission in and at the edges of the two major transmission windows (3-5μm and 8-12μm) is most important since these are the bands in which most infrared devices operate. Also, absorbed radiation will reappear as thermal energy, thereby potentially leading to nonlinear effects. For example, propagation of laser flux may be limited in a strongly nonlinear fashion, for sufficiently high power beams.

The generally low values of extinction in these spectral regions necessarily make absorption and scattering coefficients difficult to measure and model satisfactorily. A typical effect of the uncertainties in water vapor absorption alone is illustrated by the historical development of broadband infrared imaging systems, which are generally designed to operate in either the 3-5μm or 8-12μm atmospheric windows. Early design studies were based on atmospheric transmission measurements by Yates and Taylor [1], which were reduced in such a way as to omit the 10μm water continuum. Thus, these design studies predicted optimistically high performance for infrared imaging systems operating in the long wavelength window, relative to systems operating in the 3-5μm window.

While many constituents contribute to the total atmospheric attenuation, the absorption by water vapor is of greatest concern for many practical situations, especially for long-path high-visibility conditions. There is hardly a region of the infrared spectrum in which water vapor does not absorb appreciably. Moreover, of all the important gaseous absorbers, it is the least understood and most difficult to measure quantitatively. It is now generally accepted that a water vapor "continuum absorption" exists within the two major infrared windows (8-12μm and 3-5μm). However, the absorption coefficients are not known in either region with sufficient accuracy at present. In the long wavelength region laboratory and field data exist for environmental conditions and a bound has been set for the critical self-to-foreign-broadening ratio [2]. In the short wavelength region, no continuum measurements have been published for conditions typical of the natural environment. In lieu of data, continuum absorption has been extrapolated from high temperature laboratory measurements [3].

In this report we are concerned only with water vapor continuum absorption in the 3.5μm to 4.0μm spectral region. Long path (White cell) measurements on high temperature samples are reported; and for the first time, we present laboratory data obtained on samples representative of environmental conditions. These results increase the accuracy of the data base used in the modeling of the effects of the atmosphere on Army and DoD EO and HEL Systems.

The following sections present background and analytical procedures, describe the experimental techniques, and present the measurement results.

PRESENT UNDERSTANDING OF THE WATER VAPOR CONTINUA

In the following discussion, transmittance is taken to be of the form $\tau = \exp(-kL)$, where k is an absorption coefficient expressed in km^{-1} and L is the path length in km.

The available continuum absorption coefficient measurements data in both the long and short wavelength regions have been fit to a functional form of the type [2, 4]

$$k_c(\nu,T) = n_s \left(C_s(\nu,T)p_s + C_f(\nu,T)p_f \right), \tag{1}$$

where n_s is the number of water vapor molecules per cm^3, C_s and C_f have units cm^3 (km atm molecule)$^{-1}$ and are frequency (ν) and temperature (T) dependent empirical parameters which quantify, respectively, the self- and foreign-broadening contribution. p_s and p_f are, respectively, self (i.e., water vapor) and foreign gas partial pressure in atms. Often, the empirical parameters are rearranged and expressed as a self-broadening coefficient and a self-to-foreign-broadening coefficient:

$$k_c(\nu,T) = n_s \, C_s(\nu,T) \left[p_s + \frac{p_f}{B^*(\nu,t)} \right], \tag{2}$$

where $B^*(\nu,T) \equiv C_s(\nu,T)/C_f(\nu,T)$. These forms closely relate to the interpretation of the continuum as arising from the wings of distant strong lines, since early line broadening work [5] often was directed toward measuring a ratio of self-to-foreign line width parameters, $B \sim \gamma_s/\gamma_f$. For Lorentz lines, this interpretation is shown as follows. Far from the center of the i^{th} absorption line, $\nu - \nu_o^i \gg \gamma^i$ and

$$k_{wing}(\nu) \sim \sum_i \frac{S_o^i \, n_s \, \gamma^i}{(\nu - \nu_o^i)^2}, \tag{3}$$

where S_o^i and ν_o^i are, respectively, the strength and center frequency of the i^{th} absorption line. Since γ^i is the sum of self- and foreign-broadening contributions [5],

$$\gamma^i = \gamma_s^i \, p_s + \gamma_f^i \, p_f. \tag{4}$$

Then substituting Eq. (4) into Eq. (3),

$$k_{wing}(\nu) \propto n_s \sum_i \frac{S_o^i (\gamma_s^i p_s + \gamma_f^i p_f)}{(\nu - \nu_o^i)^2} \quad . \tag{5}$$

The continuum parameters may then be related to line parameters as follows:

$$C_s(\nu) \propto \sum_i \frac{S_o^i \gamma_s^i}{(\nu - \nu_o^i)^2} \quad ;$$

$$C_f(\nu) \propto \sum_i \frac{S_o^i \gamma_f^i}{(\nu - \nu_o^i)^2} \quad . \tag{6}$$

Furthermore, if the ratio γ_s^i/γ_f^i is constant across the band(s), as is often assumed for approximate work, a self-to-foreign-broadening efficiency B may be defined.

$$B = \frac{\gamma_s^i}{\gamma_f^i} \quad . \tag{7}$$

In this case, for Lorentz line shapes, the line broadening efficiency and the self-to-foreign-broadened continuum ratio have identical values:

$$\frac{C_s}{C_f} \rightarrow B \tag{8}$$

In general, however, B is not constant across the molecular band(s); and moreover, either or both the self-and foreign-broadened line shapes are not expected to be Lorentzian. Therefore, even though the interpretation of C_s/C_f as B is tempting, it can be correct only under very special circumstances (e.g., identical self- and foreign-broadened line shapes). Indeed, significant deviations of C_s/C_f from the expected B value of a band implies (for the line wing interpretation of the continuum) that the self-broadened and foreign-broadened line shapes are not the same.

If the interpretation of the continua as far wings of Lorentz lines is correct, measured absorption values should agree at least quantitatively with line-by-line calculations, within accuracy of the measured S_o^i and γ^i parameters. This is not the case [6] in the 8-12μm region,

where observed absorption is much greater than predicted for Lorentz lines. Thus the question persists as to whether non-Lorentz line wing shapes for either or both self and foreign broadening cause the continua.

Nevertheless, the magnitude and nature of the measured continua values do carry definite implications. In the 10μm region, the ratio C_f/C_s is measured to be at most .005, with a lower bound of C_f/C_s approaching zero [2]. If the lines were even nearly Lorentz the effective ratio C_f/C_s is at least an order of magnitude too small. For this reason, "dimer" theories [7] and "cluster" explanations [8] have been suggested.

In the 3.5μm to 4.1μm region, the magnitude of the absorption is compatible with what one would expect if slightly non-Lorentz shapes caused the discrepancy. Burch [3] reports a ratio $C_f/C_s \simeq .12$, a value fairly consistent with the value of $\gamma_s/\gamma_f \simeq 5$ which is characteristic of water vapor - N_2 mixtures [9]. In this region, then, an interpretation of distant line wings, for which the self-broadened shape may be slightly more super Lorentz than the foreign-broadened shape, appears more reasonable.

At the Ohio State University, some 23°C total water vapor absorption data have been obtained [10,11] from which one might infer the presence of a room temperature continuum. These data were obtained with a DF line tunable source and water vapor on mixtures prepared in a White cell.

The most extensive experiments directed toward determining a water vapor continuum in this region prior to the work reported here were elevated temperature measurements ($\geq$ 65°C) performed by Burch et al. [3]. Extrapolations were made from the high-temperature data to 23°C and to the spectral region between 3.5μm and 3.7μm. A value of C_f/C_s = 0.12 was suggested; and, lacking temperature-dependent foreign-broadened data, the temperature dependence of C_f was assumed to be that of C_s. This issue is important since the data show a strong temperature dependence.

ANALYTICAL PROCEDURE

Attempts to develop from laboratory data empirical models of the 3-5μm continuum absorption by atmospheric water vapor over the extremes of geographical and seasonal conditions are complicated by the complex nature of the absorption spectrum. In principle, there is a water vapor continuum contribution for every broadening agent with which the vapor is mixed; in addition, a pressure induced nitrogen continuum is superimposed over the water vapor continuum absorption. Also, HDO and H_2O line absorptions are superimposed over both continua.

In performing quantitative investigations, this "background" absorption must be subtracted from water vapor spectra to determine the water vapor continuum. Line absorption has a strong spectral dependence, which is usually measured by using high-resolution scanning spectroscopy and line parameter extraction techniques. Line absorption for arbitrary conditions may then be calculated by line-by-line techniques with an accuracy determined by the accuracy of individual line parameters and by the assumption of far wing line shape. The techniques for determining continuum absorption are quite unlike those required for determining line absorption. Continuum absorption does not have spectral fine structure; consequently, high-resolution and spectral scanning are not required. High-sensitivity absorption measurements are required, however, since the continuum absorption is weak and cannot be easily increased by enrichment of the sample. Ideally, the wavelengths chosen to measure continuum absorption should have minimum line contributions to minimize inaccuracy induced by background extraction. In this work, we have eliminated the pressure induced nitrogen continuum experimentally by a ratio technique which is discussed later. In one series of measurements the primary source of line background (HDO) was eliminated experimentally by using deuterium depleted water. The analytical procedure used to subtract lines from "natural" water vapor data are discussed in the following paragraphs.

The "background" line absorption coefficient $k(\nu)$ is assumed to be a superposition of Lorentz line profiles:

$$k(\nu) = \frac{1}{\pi} \sum_i \frac{S_o^i \, n_s \, \gamma^i}{(\nu - \nu_o^i)^2 + (\gamma^i)^2} \quad . \tag{9}$$

In the above, S_o is line strength per water vapor molecule, γ is the air (80% N_2 + 20% O_2) broadened Lorentz width, and n_s is the number per unit volume of the water vapor component (H_2O or HDO). The HDO number is taken to be 0.03% of the more abundant H_2O concentration, as is assumed in the Air Force Geophysics Laboratory (AFGL) data compilation [12,13].

The line width γ is the sum of contributions from self- and foreign-collision partners:

$$\gamma^i = \gamma_s^i p_s + \gamma_a^i p_a + \gamma_b^i p_b + \ldots, \tag{10}$$

where the subscript s refers to self-broadening (H_2O - H_2O or HDO - HDO collisions) and the subscripts a, b, ... refer to broadening of HDO and H_2O lines by oxygen and nitrogen and by each other. In the present

work, line broadening is caused by a mixture of foreign gases having a fixed ratio of a given foreign gas partial pressure to the total foreign gas pressure, p_f:

$$\frac{p_a}{p_f} = a \; ; \quad \frac{p_b}{p_f} = b \; ; \text{ etc.} \tag{11}$$

Consequently,

$$\gamma^i = p_s \; \gamma_s^i + p_f(a\gamma_a^i + b\gamma_b^i + \ldots)$$

$$\gamma^i = p_s \; \gamma_s^i + p_f \; \gamma_f^i \tag{12}$$

In analyzing the present data, broadening by N_2 and O_2 individually was not considered. For HDO lines, air-broadened Lorentz widths γ_f measured by Science Applications, Inc. (SAI), were used [14]. For H_2O lines, values listed in the AFGL data compilation were used [13]. Broadening of HDO lines by H_2O and vice versa was assumed to be self-broadening, even though this assumption probably represents an upper (maximum) bound. The large value of the H_2O dipole moment would seem to justify this assumption since dipole-dipole broadening varies as the product of the squares of the dipole moments, whereas resonance effects are generally of lesser importance. Accordingly, to account for self-broadening, a ratio of B = 5 was used for all H_2O and HDO collisions with air molecules.

The temperature dependences of γ_s and γ_f depend on the details of the collision process and on the population of the collision partners. If long-range forces are primarily responsible for the broadening, impact theory (e.g., Anderson theory) [15] may be used to predict a temperature dependence for each line. However, this is often not the case, particularly for foreign broadening of lines having large rotational energy. Lacking data on the lines in question and seeking to maintain uniformity with work performed elsewhere, we have assumed the usual inverse square root temperature dependence [16].

With the approximations described above, data on natural water vapor broadened by N_2/O_2 were analyzed by subtracting line absorption by using high-resolution transmission codes developed by SAI. Line wing contributions beyond 20 cm^{-1} from line center were negligible, so all calculations were truncated at this value. No attempt was made to separate self and foreign broadening of the continuum. It is noted,

however, that verification of the ratio measured by Burch as well as confirmation of the value of C_s is of considerable practical importance, since EO systems performance is sensitive to these values, except for the extremes of environmental conditions and slant range applications for which molecular absorption is not important.

The validity of this analytical approach was confirmed early in the measurements program, when 65°C DF transmission measurements near local H_2O lines indicated strength values much smaller than were listed in the AFGL data compilation at that time. More recently, the computation was updated, independently of this work, thereby giving good agreement with line absorption measured in the current work. Also, good agreement with HDO contributions is now obtained with the 1976 AFGL compilation [13], since it has been updated to include the latest HDO line parameter measurements. Measurements of D/H ratio in the water vapor samples were not performed, but measurements performed on deuterium depleted water vapor samples are consistent with the data taken with natural water vapor.

EXPERIMENTAL APPROACH AND TECHNIQUES

The experimental equipment includes absorption cells, both long-path and spectrophone, and line tunable pulsed lasers. The DF laser sources used for both the long-path absorption cell and spectrophone measurements are grating tunable pulsed Lumonics multigas lasers. Each laser is operated with an unstable resonator front reflector resulting in a doughnut-shaped, near field TEM-00 output beam.

Long-Path Absorption Cell System

The experimental setup for the DF laser measurements using the long-path cell is shown in Figure 1. The DF laser beam is made coincident with a visible He-Ne laser beam by using several flat mirrors M and one mirror M' with a central hole. Two precision-adjustable lenses are inserted in the He-Ne beam to match the effective divergence of the two lasers. The DF output wavelength is checked by inserting a lens and spectrum analyzer into the DF laser beam. After the DF laser beam traverses the length of the laboratory, it is collected by mirror CM1. Mirror CM2 is used to collimate the DF and He-Ne laser beams to 5 mm diameter before entering the 21-m absorption cell. An optical flat B is used to split a portion of the beam to the cell input detector ID. The remaining portion of the beam passes through window W. A multipath through the cell is obtained by using White-type reflective optics. The cell output beam is detected by the cell output detector OD. Teflon membrane filters F are placed in front of the detectors to diffuse the laser beam. Apertures A are placed in front of the detectors to prevent detector saturation. A more detailed account is given elsewhere [17].

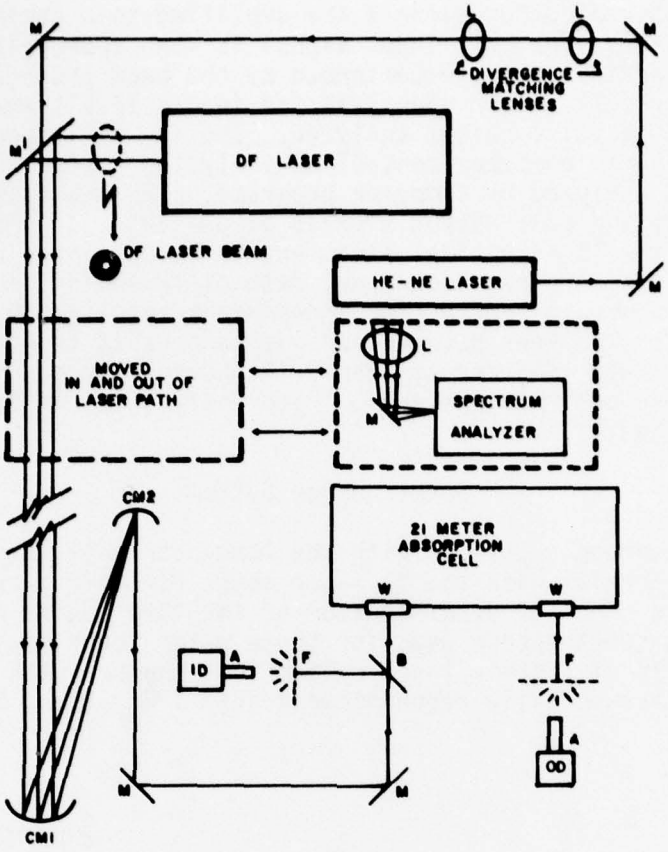

Figure 1. Experimental arrangement.

For the water vapor absorption measurements, a known amount of water was introduced into the 21-m cell under vacuum and allowed to evaporate. The equilibrium pressure was measured by a capacitance manometer prior to injecting an 80%/20% mixture of N_2/O_2 to buffer the water vapor to 760 torr total pressure. After buffering the water vapor partial pressure was monitored by using a dewpoint hygrometer. Measurements were performed at two temperatures, 23° and 65°C. The reference cell condition required for long-path cell measurements was a 760 torr 80%/20% mixture of N_2/O_2 with corresponding amount of water vapor pressure replaced by O_2 since N_2 absorbs at several DF frequencies. Additional measurement technique details are given elsewhere [18,19].

The signal analyzing system for the long-path absorption cell is described in the literature [18]. The DF laser pulses are submicrosecond in duration and the pulse repetition frequency is 0.3 Hz. Both

the cell input and output signals are amplified to a nominal 7-V level for digitization. The cell input signal is then appropriately delayed to match the optical delay experienced by the beam propagated through the absorption cell. Each signal is fed into a 14-bit analog-to-digital converter and is pulse-height analyzed. The two digitized signals are then sent to a minicomputer controlled analyzing system where they are displayed and analyzed by computer programs. The real-time display of the cell input and cell output signals allows detector-amplifier nonlinearities as well as optical alignment to be corrected during measurements. In addition a new technique, path differencing, is used in data acquisition to obtain nearly time independent results [19]. The technique uses rapid changes between two pathlengths to time average short-term and eliminate long-term system drift normally encountered in long-path absorption cell measurements. Path differences of from 1008 to 1512 m were used.

Spectrophone System

In the spectrophone system as with the long-path cell, a He-Ne laser beam is made coaxial with the DF laser beam. In this case though, a calorimeter is used for determination of the laser pulse energy. The pulsed source spectrophone used for these water vapor measurements consists basically of a semi-closed cylindrical chamber with a dominant longitudinal acoustically resonant mode near 1 kHz (Fig. 2).

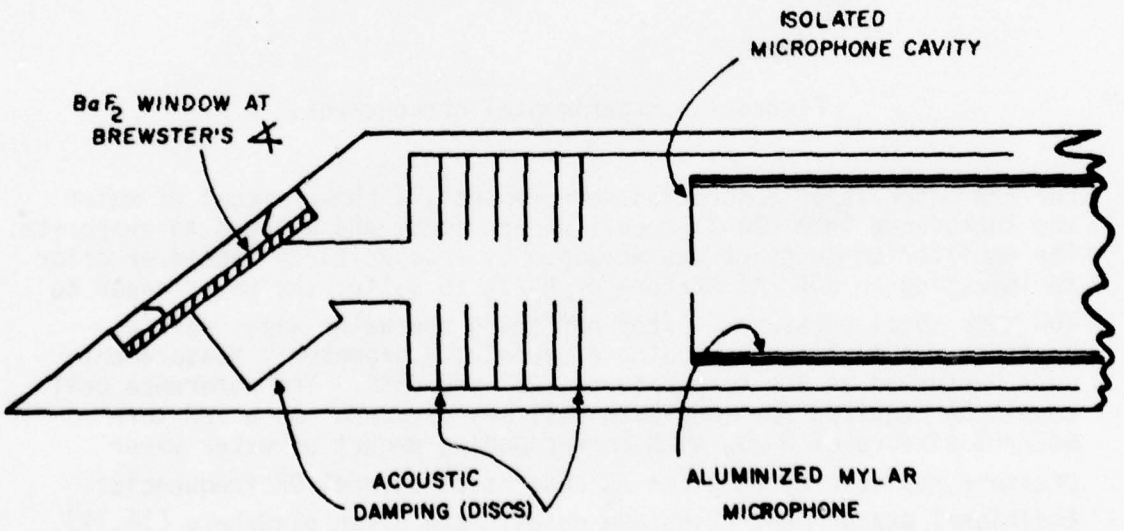

Figure 2. Schematic drawing of pulsed source spectrophone.

This chamber is positioned within another cylindrical chamber made of stainless steel which is evacuable and bakeable. The spectrophone entrance and exit windows are located in the ends of this outer cylinder and are thus well removed from the entrance and exit apertures of the interior resonant chamber. This arrangement and acoustical dampers serve to avoid contributions to the spectrophone output signal due to the window absorption. An aluminum coated mylar diaphragm, forming a complete circular cylinder at the perimeter of the inner chamber, serves as a capacitance microphone sensor for the absorption signal. The time resolved signals from a number of laser pulses were averaged on a point by point basis by using a PAR signal "eductor," and the developing signal was displayed on an oscilloscope and plotted for analysis. The set of relative absorption values was then referenced to a known absorption using methane as a trace gas in the same N_2/O_2 buffer gas. Both physical design of the pulsed source spectrophone and methods of signal treatment have been discussed elsewhere [20,21].

Several spectrophone measurements were made to determine whether (1) extraneous sources or (2) impurities contribute to the water vapor absorption signal. Pure nitrogen was used to verify the absence of extraneous sources since nitrogen absorbs in a continuum which is very weak at the shorter wavelength end of the DF laser spectrum ($< 10^{-4} km^{-1}$ at 2800 cm^{-1}). No absorption was detected; therefore, we conclude that no extraneous sources exist. The approach with regard to the impurities was less direct. The same singly distilled water (metallic still) was used for both spectrophone and White cell measurements. In addition, several sets of spectrophone measurements were made for each of two other water samples which were prepared in a specially designed, all-glass still. This still forms a closed system and is purged with argon during the distillation process. The two samples prepared in this still were singly and multiply distilled. The results were not significantly different for the three conditions in spite of the differential distillation of the components.

DISCUSSION OF EXPERIMENTAL RESULTS

65°C Water Vapor Absorption

As stated above, measurements were made at temperatures of 65° and 23°C. The 65°C measurements were made to allow a comparison with the water vapor continuum results of Burch et al. [3] near their experimental conditions. A direct comparison of the total water absorption as measured here by using the White cell system with the latest calculation [13] is given in Fig. 3. The overall agreement between the measurement and the prediction is good. The disagreements between the two results occur mainly in the region near 2800 cm^{-1} where HDO line absorption is large.

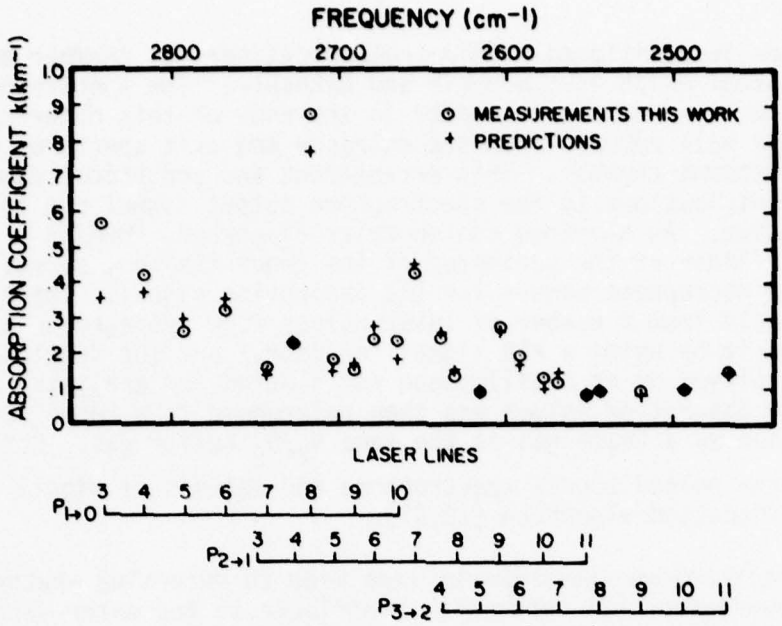

Figure 3. Total water vapor absorption measurements and predictions at 65°C with 72 torr water vapor buffered to 760 torr.

This set of measurements has been used to infer the water continuum. The inferred values were obtained by subtracting calculated HDO and H_2O line contributions from the measured total water absorption values. The results are shown in Fig. 4 and Table 1 along with the continuum predicted from Burch's high-temperature measurements. The present results and the Burch prediction are in substantial agreement between 2450 and 2700 cm^{-1}; however, the inferred continuum values have considerable scatter beyond 2700 cm^{-1}.

The large apparent scatter in the inferred continuum does not reflect measurement precision; the precision is indicated by the error bar in Fig. 4. The scatter is caused by uncertainty in the line absorption coefficients which are subtracted from the measured data to infer the continuum. At some frequencies, the line absorption dominates the total (line plus continuum) absorption as indicated in Table 1. Burch did not directly measure the self-broadened continuum at this temperature beyond 2650 cm^{-1}. By using his measured results between 2400 and 2650 cm^{-1} and extrapolation scheme (discussed later), the continuum between 2650 and 2820 cm^{-1} can be modeled [3]. The error limit on the Burch predictions is $\pm$50%.

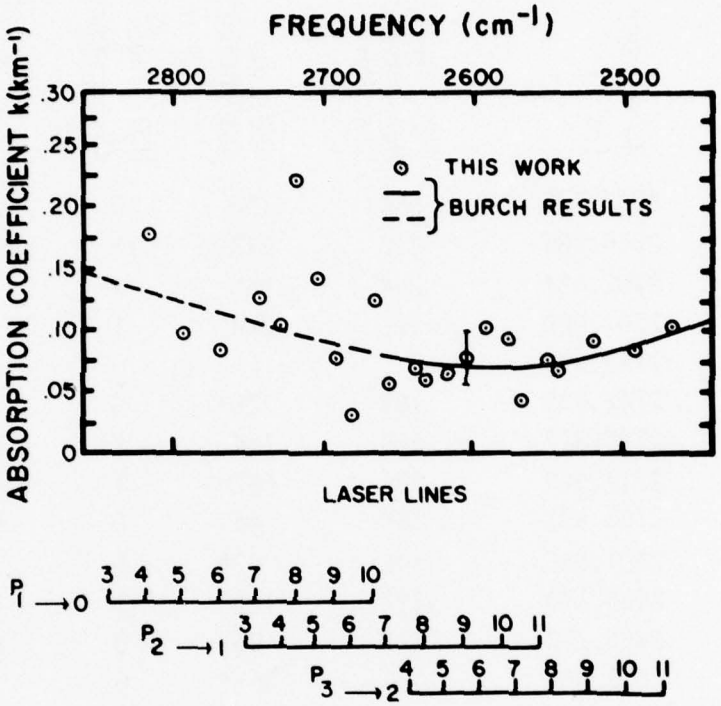

Figure 4. Inferred continuum this work at 65°C with 72 torr water vapor buffered to 760 torr compared to Burch results. Burch results are as follows: Solid curve based on 65°C self-broadened data and higher temperature foreign-broadened extrapolation; dashed curve based on extrapolation of higher temperature self- and foreign-broadened data.

TABLE 1

WATER VAPOR ABSORPTION COEFFICIENTS (km^{-1}) x 10^3 WITH 72 TORR WATER VAPOR AT 65°C BUFFERED TO 760 TORR

Laser Line	Wavenumber (cm^{-1})	Total Water Measurement This Work	HDO Line Absorption[13]	H_2O Line Absorption[13]	Water Continuum This Work	Burch Water Continuum[3]
$P_1(3)$	2839.796	564	198	6	360	138
$P_1(4)$	2816.385	410	222	13	175	131
$P_1(5)$	2792.434	264	165	2	97	123
$P_1(6)$	2767.968	313	228	1	84	115
$P_2(3)$	2750.096					
$P_1(7)$	2742.988	152	25*	0	127	107
$P_2(4)$	2727.312	218	114	2	102	101
$P_1(8)$	2717.543	883	662*	1	220	98
$P_2(5)$	2703.993	185	46	0	139	93
$P_1(9)$	2691.605	145	62*	5	78	89
$P_2(6)$	2680.173	227	195	3	29	86
$P_1(10)$	2665.218	221	96	0	125	82
$P_2(7)$	2655.861	424	367*	0	57	80
$P_3(4)$	2640.075	236	164	0	72	77
$P_2(8)$	2631.067	124	17	44	62	75
$P_3(5)$	2617.389	94	23	0	71	72
$P_2(9)$	2605.808	267	187*	0	80	70
$P_3(6)$	2594.201	190	83	4	103	69
$P_2(10)$	2580.102	120	29	0	91	69
$P_3(7)$	2570.523	111	64	1	46	70
$P_2(11)$	2553.954	83	8	0	75	72
$P_3(8)$	2546.375	92	20	1	71	74
$P_3(9)$	2521.769	95	3	1	91	81
$P_3(10)$	2496.722	96	1	8	87	90
$P_3(11)$	2471.245	137	0	33	104	100

*Includes updated HDO values from references 14 and 22.

23°C Water Vapor Absorption

Natural water vapor absorption coefficients have been measured in both the White cell and in the spectrophone, while deuterium-depleted water vapor values have been measured in the White cell. The natural water vapor absorption coefficients measured in the White cell for 25 DF laser lines are given in column 3 of Table 2. These results were obtained at 23°C with a water vapor pressure of 14.3 torr and buffered to a total pressure of 760 torr by an 80%/20% mixture of N_2/O_2. Since the absorption was referenced to that of an 80%/20% mixture of N_2/O_2, the N_2 pressure induced continuum absorption was subtracted out experimentally. The above corresponds to the midlatitude summer (MLS) atmospheric model which has become the standard for such measurements. Table 2 also shows calculated values for the various component absorption contributions. The theoretical line absorptions and calculations are based on AFGL absorption line parameter compilations [13] (column 4 of Table 2). HDO calculations (indicated by asterisks) have been modified based on recent SAI spectral measurements [14,22]. The continuum predictions (column 6 of Table 2) are based on Burch's measurements [3]. Since his measurements were made between 65°C and 155°C, he obtained the continuum values by extrapolating the higher temperature data to 23°C.

The extrapolation procedure used by Burch, et al. [3] to obtain the 23°C air-broadened water vapor continuum is described completely in reference 3. Since this reference is not readily available, the procedure will be discussed briefly. Several wavelengths were chosen in the 3.5μm to 4.1μm region where normal water line absorption was a minimum. Absorption measurements were made at elevated temperatures of 65°, 111°, and 155°C because sufficient water vapor resulting in measurable absorption could be introduced into their absorption cell. Pure water vapor absorption (i.e., with no buffering by other atmospheric gases) was measured as a function of water vapor pressure. The results were given in terms of the self-broadened water continuum (assumed to be far wing) empirical parameter C_s which is related to the absorption coefficient k as follows [see Eq. (1)]:

$$k = n_s C_s p \qquad (13)$$

where p is the water vapor pressure. k_s was found to vary linearly with water vapor pressure and C_s was found to be proportional to exp(constant/θ), where θ is the temperature in Kelvin. Next, the foreign-broadened water continuum absorption coefficient C_{N_2} was measured. Measurements were made at 155°C with 2 atm of water vapor buffered by nitrogen to 4.5, 5.7, 7.5, and 10 atm. From these measurements, a measure of C_{N_2} was obtained which relates to the self- and foreign-broadened water vapor continuum absorption coefficient as

TABLE 2

NATURAL WATER VAPOR ABSORPTION COEFFICIENTS (km^{-1}) x 10^3
WITH 14.3 TORR WATER VAPOR AT 23°C BUFFERED TO 760 TORR

Laser Line	Wavenumber (cm^{-1})	Total Water Measurement This Work	H_2O, HDO Line Contribution[13]	Water Continuum This Work	Burch Water Continuum[3]	Total Water Measurement OSU[28]
$P_1(3)$	2839.796	145	53	92	39	
$P_1(4)$	2816.385	143	48	95	36	
$P_1(5)$	2792.434	95	35	60	33	
$P_1(6)$	2767.968	111	51	60	31	
$P_2(3)$	2750.096	63	20	43	29	
$P_1(7)$	2742.988	69	5*	64	28	
$P_2(4)$	2727.312	69	24	45	27	
$P_1(8)$	2717.543	167	120*	47	26	
$P_2(5)$	2703.993	61	7	54	24	
$P_1(9)$	2691.605	66	14*	52	23	
$P_2(6)$	2680.173	93	43	50	22	75
$P_1(10)$	2665.218	78	20	58	21	
$P_2(7)$	2665.861	129	78*	51	20	103
$P_3(4)$	2640.075	78	36	42	19	
$P_2(8)$	2631.067	44	8	36	19	38
$P_3(5)$	2617.389	44	4	40	18	
$P_2(9)$	2605.808	67	32*	35	17	
$P_3(6)$	2594.201	64	13	51	17	59
$P_2(10)$	2580.102	43	4	39	17	
$P_3(7)$	2570.523	63	8	55	18	35
$P_2(11)$	2553.954	52	1	51	18	
$P_3(8)$	2546.375	41	3	38	19	29
$P_3(9)$	2521.769	41	0	41	21	
$P_3(10)$	2496.722	44	1	43	23	
$P_3(11)$	2471.245	38	4	34	26	

*Includes updated HDO values of SAI from references 14 and 22.

shown in Eq. (1). Assuming the nitrogen broadening to be the same as oxygen broadening, the water vapor continuum absorption due to atmospheric water vapor can be obtained by extrapolation of the above measurements. The results of Burch's measurements and his extrapolation scheme (i.e., the extrapolated value of C_s at 23°C with the assumption that the ratio of C_{N_2} to C_s at 155°C is the same as that at 23°C for 14.3 torr of water vapor in a 760 torr total pressure atmosphere) are shown by the dashed curve in Fig. 5 with an estimated ±65% error limit. A similar approach, with regard to the foreign broadening, was followed for Burch's 65°C water vapor absorption data presented earlier.

Inferred continuum absorption coefficients from the present measurements are calculated by subtracting theoretical HDO and H_2O line absorption coefficients from measured total water absorption coefficients. These are given in column 5 of Table 2.

A more direct measure of the water vapor continuum was made by using HDO depleted water [23,24]. Water vapor absorption in this spectral region is comprised of the water vapor continuum, substantial HDO line absorption, and weak H_2O line absorption. By using an HDO depleted water sample the need to subtract absorption line contributions was eliminated for about one-half of the laser lines used and was only a few percent of the total absorption for the remaining lines. An analysis of the deuterium depleted water sample indicated 2% the natural HDO concentration [25]. The results of these measurements with 24 DF laser lines are given in Table 3. HDO absorption has been measured [26] with a spectrophone and these measurements show general agreement with the predictions. Thus, for an HDO depleted water vapor sample, the water vapor continuum level is not significantly altered by the decrease in the HDO molecules.

The total natural water vapor absorption was also measured with a spectrophone. From these results, an inferred continuum was obtained in the same manner as that used for the White cell measurements. The spectrophone system was calibrated by using known concentrations of methane and measured methane absorption coefficients [21,27].

The inferred and directly measured (HDO-depleted) water vapor continuum values at 23°C are given in Table 4 with the RMS uncertainties. The uncertainties shown for the average values listed in column 5 of Table 4 represent typical measurement set RMS reproducibilities. The uncertainties of the average values for laser line at the beginning and ending of series are larger than others probably due to weaker laser emission. The average of the three sets of data is shown as circles in Fig. 5 along with the continuum extrapolated from the Burch measurement and published measurements by the Ohio State University (OSU) group [11,28] (see column 7 of Table 2). The solid curve in Fig. 5 is a least squares fit with an estimated uncertainty of 25%. The present results indicate a water continuum roughly twice as large as that of

TABLE 3

HDO DEPLETED WATER VAPOR AND WATER LINE ABSORPTION COEFFICIENTS
(km^{-1}) x 10^3 WITH 14.3 TORR WATER VAPOR AT 23°C BUFFERED TO 760 TORR

Laser Line	Frequency (cm^{-1})	HDO Depleted Water Vapor Absorption Coefficients*	$HDO + H_2O$ Line[13] Absorption Coefficients
$P_1(3)$	2839.791	117 ± 2	-
$P_1(4)$	2816.380	128 ± 4	3
$P_1(5)$	2792.434	91 ± 15	1
$P_1(6)$	2767.968	82 ± 10	1
$P_2(3)$	2750.093	76 ± 7	-
$P_1(7)$	2742.997	65 ± 12	-
$P_2(4)$	2727.308	90 ± 6	1
$P_1(8)$	2717.538	81 ± 6	2
$P_2(5)$	2703.998	70 ± 5	-
$P_1(9)$	2691.608	50 ± 2	1
$P_2(6)$	2680.178	53 ± 9	1
$P_1(10)$	2665.218	46 ± 18	-
$P_2(7)$	2655.863	54 ± 7	2
$P_3(4)$	2640.075	30 ± 3	1
$P_2(8)$	2631.066	33 ± 10	5
$P_3(5)$	2617.386	47 ± 4	-
$P_2(9)$	2605.806	35 ± 6	1
$P_3(6)$	2594.197	49 ± 11	1
$P_2(10)$	2580.095	25 ± 13	-
$P_3(7)$	2570.522	43 ± 10	-
$P_2(11)$	2553.951	42 ± 7	-
$P_3(8)$	2546.373	33 ± 10	-
$P_3(9)$	2521.769	43 ± 11	-
$P_3(11)$	2471.243	74 ± 6	4

*The uncertainties shown are RMS measurement uncertainties, i.e., the precision of the measurement.

TABLE 4

WATER VAPOR CONTINUUM ABSORPTION COEFFICIENTS

$(km^{-1}) \times 10^3$ FOR 14.3 TORR WATER VAPOR AT 23°C BUFFERED TO 760 TORR

Laser Line	Natural Water Vapor Spectrophone*	Natural Water Vapor White Cell*	HDO Depleted Water Vapor White Cell*	Average †
$P_1(3)$		92 ± 4	117 ± 2	105 ± 18
$P_1(4)$		95 ± 10	125 ± 4	110 ± 21
$P_1(5)$	96 ± 5	60 ± 7	90 ± 15	82 ± 19
$P_1(6)$	68 ± 5	60 ± 4	81 ± 10	70 ± 11
$P_2(3)$		43 ± 10	76 ± 7	60 ± 23
$P_1(7)$	78 ± 4	64 ± 6	65 ± 12	69 ± 8
$P_2(4)$	62 ± 6	45 ± 5	89 ± 6	65 ± 22
$P_1(8)$	75 ± 7	47 ± 11	79 ± 6	67 ± 17
$P_2(5)$	57 ± 3	54 ± 7	70 ± 5	60 ± 9
$P_1(9)$	48 ± 2	52 ± 8	49 ± 2	50 ± 2
$P_2(6)$	49 ± 3	50 ± 8	52 ± 9	50 ± 2
$P_1(10)$	28 ± 2	58 ± 8	46 ± 18	44 ± 15
$P_2(7)$	48 ± 5	51 ± 6	52 ± 7	50 ± 2
$P_3(4)$	19 ± 2	42 ± 10	29 ± 3	30 ± 12
$P_2(8)$	38 ± 4	36 ± 7	28 ± 10	34 ± 5
$P_3(5)$	42 ± 3	40 ± 3	47 ± 4	43 ± 4
$P_2(9)$	37 ± 4	35 ± 9	34 ± 6	35 ± 2
$P_3(6)$	46 ± 2	51 ± 11	48 ± 11	48 ± 3
$P_2(10)$	39 ± 4	39 ± 20	25 ± 13	34 ± 8
$P_3(7)$	39 ± 2	55 ± 10	43 ± 10	46 ± 8
$P_2(11)$		51 ± 8	42 ± 7	47 ± 6
$P_3(8)$	36 ± 3	38 ± 10	33 ± 10	36 ± 3
$P_3(9)$	40 ± 3	41 ± 7	43 ± 11	41 ± 2
$P_3(10)$		43 ± 12		43 ± 12
$P_3(11)$		34 ± 15	70 ± 6	52 ± 25

*The uncertainties shown are RMS measurement uncertainties, i.e., the precision of the measurement.

†The uncertainties shown are RMS measurement uncertainties, i.e., the reproducibility of the measurement set.

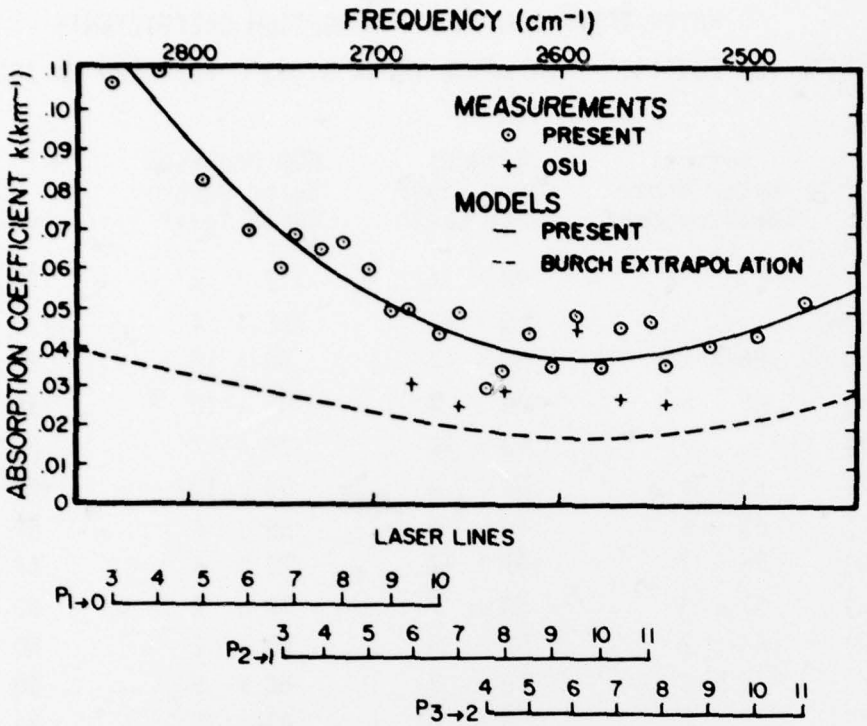

Figure 5. Comparison of measured water continuum at 23°C with 14.3 torr water vapor buffered to 760 torr.

Burch near 3.8μm, and about a factor of 3 greater near 3.5μm. The inferred OSU continuum values indicate a continuum level slightly less than present values.

The Burch measurements of water vapor continuum did not include an analysis of how the expected error bounds on the self- and foreign-induced coefficients (C_s and C_f) influence the error in the total water continuum absorption coefficient k_c. A Monte Carlo technique was used for evaluating the combination of the various errors, including the effects of temperature extrapolation [29].

Briefly, the Monte Carlo technique employed selects statistically, from appropriate distribution functions, values for all the variables which have an associated uncertainty. The values for these variables are then combined, according to the governing equation, to evaluate a statistical sample for k_c. This procedure is repeated several hundred times (each time using new randomly generated numbers), until sufficient statistics are accumulated to evaluate accurately the total uncertainty in k_c.

Results of this analysis on Burch's data and a comparison with present results are shown in Fig. 6. The present values are well above the closest error bound. It is concluded that the high-temperature measurements agree quite well with the Burch measurements, but the 23°C extrapolation of Burch underestimates the continuum by at least a factor of 2.

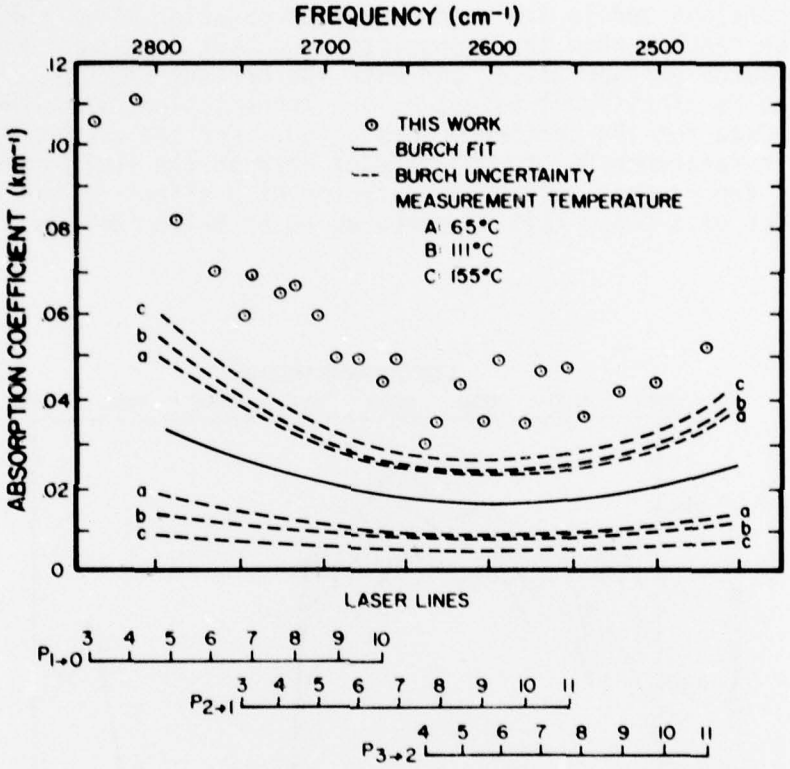

Figure 6. Comparison of water continuum absorption measurements: Burch's uncertainty bounds and this work measurements. Temperature = 23°C, pressure H_2O = 14.3 torr, total pressure = 760 torr.

IMPACT OF RESULTS ON MODELING

An understanding of the water vapor continua in both the 3.0μm to 5.0μm and the 8.0μm to 12.0μm regions is important for predicting performance of high-energy laser (HEL) devices and for performance evaluations of broadband systems.

The significance of determining accurately the water vapor continuum absorption in the 3.0μm to 5.0μm region is indicated in analysis of performance of thermal imaging systems. Comparisons have been made of relative performance between forward-looking infrared (FLIR) devices designed to operate in the 3.0μm to 5.0μm and 8.0μm to 12.0μm windows [30]. Transmission predictions, and therefore, FLIR performance, are impacted by the magnitude of the self- and foreign-broadening coefficients, their relative magnitude and their temperature dependence. The effect at the shorter wavelength window is shown in Fig. 7 where various continua models are used in the propagation model LOWTRAN 3A [31]. The results show the transmission without continuum absorption, with the Burch extrapolation, and with the present results. As can be seen there is significant effect on the transmission depending on what value is used for the continuum absorption. For the conditions considered in reference 29, the difference between the Burch continuum value and the present values has a factor of 5 effect on the relative performance of a 3-5μm FLIR as compared to an 8-12μm device.

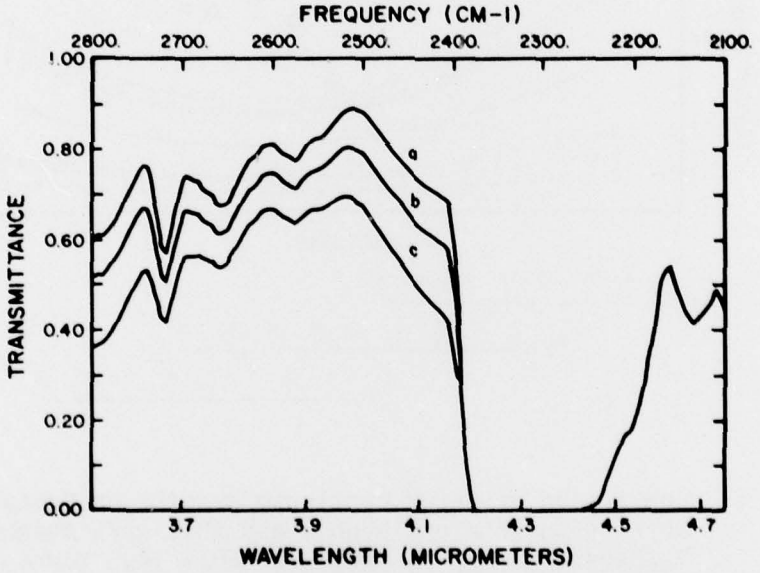

Figure 7. Calculated spectral atmospheric transmission for various water continuum models: tropical model atmosphere, 8.5 km visibility, 0.75 km altitude, 5 km range; (a) zero continuum, (b) continuum extrapolated from measurements of Burch, (c) continuum measured this work.

REFERENCES

1. Yates, H. W., and J. H. Taylor, 1960, "Infrared Transmission of the Atmosphere," NRL Report 5453, AD 240180.

2. Roberts, R. E., J. E. A. Selby, and L. M. Biberman, 1976, "Infrared Continuum Absorption by Atmospheric Water Vapor in the 8-12μm Window," Appl. Opt. 15:2085.

3. Burch, D. E., D. A. Gryvnak, and J. D. Pembrook, 1971, "Investigation of the Absorption of Infrared Radiation by Atmospheric Gases: Water, Nitrogen, Nitrous Oxide," AFCRL-71-0124.

4. Burch, D. E., D. A. Gryvnak, and J. D. Pembrook, 1970, "Investigation of the Absorption of Infrared Radiation by Atmospheric Gases," AFCRL-70-0373.

5. Burch, D. E., E. B. Singleton, and D. Williams, 1962, "Absorption Line Broadening in the Near Infrared," Appl. Opt. 1:359.

6. Farmer, C. B., 1967, "Extinction Coefficients and Computed Spectra for the Rotational Band of Water Vapor," EMI Electronics, LTD, Report DMP 2780.

7. Varanasi, P., S. Chou, and S. S. Penner, 1968, "Absorption Coefficients for Water Vapor in the 600-1000 cm^{-1} Region," J. Quant. Spectrosc. Radiat. Transfer 8:1537.

8. Carlon, H. R., 1971, "Models for Infrared Emissions of Water Vapor/Aerosol Mixtures," Appl. Opt. 10:2297.

9. Benedict, W. S., and L. D. Kaplan, 1959, "Calculation of Line Widths in H_2O-N_2 Collisions," J. Chem. Phys. 30:388.

10. Damon, E. K., J. C. Peterson, F. S. Mills, and R. K. Long, 1975, "Spectrophone Measurement of the Water Vapor Continuum at DF Laser Frequencies," RADC-TR-75-203. OSU Report ESL 4045-1.

11. Mills, F. S., R. K. Long, and E. K. Damon, 1975, "Laser Absorption Studies," RADC-TR-75-289. OSU Report ESL 4054-2.

12. Field data obtained after completion of this work by the Naval Research Laboratory using the gas filter correlation technique indicates that a value of 0.02% of the H_2O concentration is more appropriate. The reason for this is not clear, nor is it clear that this lower value is more appropriate for the sample used in this work. This will be investigated during the course of our ongoing measurements.

13. McClatchey, R. A., W. S. Benedict, S. A. Clough, D. E. Burch, R. E. Calfee, K. Fox, L. S. Rothman, and J. S. Garing, 1973, "AFCRL Atmospheric Absorption Line Parameter Compilation," AFCRL-TR-73-0096. Analyses were performed using the data tape published January 1976.

14. Woods, D. R., W. Flowers, R. E. Meredith, T. W. Tuer, and J. P. Walker, 1977, "DF Laser Propagation Analysis," Science Applications, Inc., Report SAI-77-001-AA.

15. Anderson, P. W., 1949, "Pressure Broadening in the Microwave and Infra-Red Regions," Phys. Rev. 76:647.

16. Penner, S. S., 1959, Quantitative Molecular Spectroscopy and Gas Emissivities, Addison-Wesley, Reading, Massachusetts, p. 28.

17. White, K. O., and W. R. Watkins, 1975, "Absorption of DF Laser Radiation by Propane and Butane," US Army Electronics Command Report, ECOM-5563, AD A012169.

18. White, K. O., G. T. Wade, and S. A. Schleusener, 1973, "The Application of Minicomputers in Laser Atmospheric Experiments," Proc. IEEE 61:1596.

19. Watkins, W. R., 1976, "Path Differencing: An Improvement to Multipass Absorption Cell Measurements," Appl. Opt. 15:16.

20. Bruce, C. W., 1976, "Development of Spectrophones for CW and Pulsed Radiation Sources," US Army Electronics Command Report, ECOM-5802.

21. Bruce, C. W., B. Z. Sojka, B. G. Hurd, W. R. Watkins, K. O. White, and Z. Derzko, 1976, "Application of Pulsed-Source Spectrophone to Absorption by Methane at DF Laser Wavelengths," Appl. Opt. 15:2970.

22. Woods, D. R., R. E. Meredith, F. G. Smith, and T. W. Tuer, 1975, "High Resolution Spectral Survey of Molecular Absorption in the DF Laser Region: Measurements and Calculations," Rome Air Development Center, Griffiss AFB, NY, RADC-TR-75-180.

23. The HDO depleted water sample was obtained from Science Applications, Inc., Ann Arbor, Michigan.

24. Watkins, W. R., and K. O. White, 1977, "Water Vapor Continuum Absorption Measurements (3.5-4.0μm) Using HDO Depleted Water," Opt. Letters 1:31.

25. Thurston, W. M., Atomic Energy of Canada, General Chemistry Branch, Chalk River, Ontario, Canada, Private Communication (1976).

26. Bruce, C. W., and K. O. White, 1976, "Absorption by HDO at DF Laser Wavelengths," J. Opt. Soc. Am. 66:1088A.

27. Spencer, D. J., G. C. Denault, and H. H. Takimoto, 1975, "Atmospheric Gas Absorption at DF Laser Wavelengths," Appl. Opt. 13:2855.

28. Mills, F. S., "Absorption of Deuterium Fluoride Laser Radiation by the Atmosphere," Ohio State University Ph D Dissertation, Electroscience Laboratory 4054-3.

29. Tuer, T., SAI, Ann Arbor, Michigan, private communication, 1976.

30. Tuer, T. W., 1977, "Thermal Imaging Systems Relative Performance: 3-5 μm Versus 8-12 μm," AFAL-TR-76-217.

31. Selby, J. E. A., and R. M. McClatchey, 1975, "Atmospheric Transmittance from 0.25 to 28.5 μm: Computer Code Lowtran 3," AFCRL-TR-75-0255.

ATMOSPHERIC SCIENCES RESEARCH PAPERS

1. Lindberg, J.D., "An Improvement to a Method for Measuring the Absorption Coefficient of Atmospheric Dust and other Strongly Absorbing Powders, " ECOM-5565, July 1975.
2. Avara, Elton, P., "Mesoscale Wind Shears Derived from Thermal Winds," ECOM-5566, July 1975.
3. Gomez, Richard B., and Joseph H. Pierluissi, "Incomplete Gamma Function Approximation for King's Strong-Line Transmittance Model," ECOM-5567, July 1975.
4. Blanco, A.J., and B.F. Engebos, "Ballistic Wind Weighting Functions for Tank Projectiles," ECOM-5568, August 1975.
5. Taylor, Fredrick J., Jack Smith, and Thomas H. Pries, "Crosswind Measurements through Pattern Recognition Techniques," ECOM-5569, July 1975.
6. Walters, D.L., "Crosswind Weighting Functions for Direct-Fire Projectiles," ECOM-5570, August 1975.
7. Duncan, Louis D., "An Improved Algorithm for the Iterated Minimal Information Solution for Remote Sounding of Temperature," ECOM-5571, August 1975.
8. Robbiani, Raymond L., "Tactical Field Demonstration of Mobile Weather Radar Set AN/TPS-41 at Fort Rucker, Alabama," ECOM-5572, August 1975.
9. Miers, B., G. Blackman, D. Langer, and N. Lorimier, "Analysis of SMS/GOES Film Data," ECOM-5573, September 1975.
10. Manquero, Carlos, Louis Duncan, and Rufus Bruce, "An Indication from Satellite Measurements of Atmospheric CO2 Variability," ECOM-5574, September 1975.
11. Petracca, Carmine, and James D. Lindberg, "Installation and Operation of an Atmospheric Particulate Collector," ECOM-5575, September 1975.
12. Avara, Elton P., and George Alexander, "Empirical Investigation of Three Iterative Methods for Inverting the Radiative Transfer Equation," ECOM-5576, October 1975.
13. Alexander, George D., "A Digital Data Acquisition Interface for the SMS Direct Readout Ground Station — Concept and Preliminary Design," ECOM-5577, October 1975.
14. Cantor, Israel, "Enhancement of Point Source Thermal Radiation Under Clouds in a Nonattenuating Medium," ECOM-5578, October 1975.
15. Norton, Colburn, and Glenn Hoidale, "The Diurnal Variation of Mixing Height by Month over White Sands Missile Range, N.M," ECOM-5579, November 1975.
16. Avara, Elton P., "On the Spectrum Analysis of Binary Data," ECOM-5580, November 1975.
17. Taylor, Fredrick J., Thomas H. Pries, and Chao-Huan Huang, "Optimal Wind Velocity Estimation," ECOM-5581, December 1975.
18. Avara, Elton P., "Some Effects of Autocorrelated and Cross-Correlated Noise on the Analysis of Variance, " ECOM-5582, December 1975.
19. Gillespie, Patti S., R.L. Armstrong, and Kenneth O. White, "The Spectral Characteristics and Atmospheric CO2 Absorption of the Ho^{+3}:YLF Laser at 2.05μm," ECOM-5583, December 1975.
20. Novlan, David J. "An Empirical Method of Forecasting Thunderstorms for the White Sands Missile Range," ECOM-5584, February 1976.
21. Avara, Elton P., "Randomization Effects in Hypothesis Testing with Autocorrelated Noise," ECOM-5585, February 1976.
22. Watkins, Wendell R., "Improvements in Long Path Absorption Cell Measurement," ECOM-5586, March 1976.
23. Thomas, Joe, George D. Alexander, and Marvin Dubbin, "SATTEL — An Army Dedicated Meteorological Telemetry System," ECOM-5587. March 1976.
24. Kennedy, Bruce W., and Delbert Bynum, "Army User Test Program for the RDT&E-XM-75 Meteorological Rocket," ECOM-5588, April 1976.

25. Barnett, Kenneth M., "A Description of the Artillery Meteorological Comparisons at White Sands Missle Range, October 1974 - December 1974 ('PASS' - Prototype Artillery [Meteorological] Subsystem)," ECOM-5589, April 1976.
26. Miller, Walter B., "Preliminary Analysis of Fall-of-Shot From Project 'PASS'," ECOM-5590, April 1976.
27. Avara, Elton P., "Error Analysis of Minimum Information and Smith's Direct Methods for Inverting the Radiative Transfer Equation," ECOM-5591, April 1976.
28. Yee, Young P., James D. Horn, and George Alexander, "Synoptic Thermal Wind Calculations from Radiosonde Observations Over the Southwestern United States," ECOM-5592, May 1976.
29. Duncan, Louis D., and Mary Ann Seagraves, "Applications of Empirical Corrections to NOAA-4 VTPR Observations," ECOM-5593, May 1976.
30. Miers, Bruce T., and Steve Weaver, "Applications of Meterological Satellite Data to Weather Sensitive Army Operations,"ECOM-5594, May 1976.
31. Sharenow, Moses, "Redesign and Improvement of Balloon ML-566," ECOM-5595, June, 1976.
32. Hansen, Frank V., "The Depth of the Surface Boundary Layer," ECOM-5596, June 1976.
33. Pinnick, R.G., and E.B. Stenmark, "Response Calculations for a Commercial Light-Scattering Aerosol Counter," ECOM-5597, July 1976.
34. Mason, J., and G.B. Hoidale, "Visibility as an Estimator of Infrared Transmittance," ECOM-5598, July 1976.
35. Bruce, Rufus E., Louis D. Duncan, and Joseph H. Pierluissi, "Experimental Study of the Relationship Between Radiosonde Temperatures and Radiometric-Area Temperatures," ECOM-5599, August 1976.
36. Duncan, Louis D., "Stratospheric Wind Shear Computed from Satellite Thermal Sounder Measurements," ECOM-5800, September 1976.
37. Taylor, F., P. Mohan, P. Joseph and T. Pries, "An All Digital Automated Wind Measurement System," ECOM-5801, September 1976.
38. Bruce, Charles, "Development of Spectrophones for CW and Pulsed Radiation Sources," ECOM-5802, September 1976.
39. Duncan, Louis D., and Mary Ann Seagraves,"Another Method for Estimating Clear Column Radiances," ECOM-5803, October 1976.
40. Blanco, Abel J., and Larry E. Taylor, "Artillery Meteorological Analysis of Project Pass," ECOM-5804, October 1976.
41. Miller, Walter, and Bernard Engebos," A Mathematical Structure for Refinement of Sound Ranging Estimates," ECOM-5805, November, 1976.
42. Gillespie, James B., and James D. Lindberg, "A Method to Obtain Diffuse Reflectance Measurements from 1.0 to 3.0 μm Using a Cary 171 Spectrophotometer," ECOM-5806, November 1976.
43. Rubio, Roberto, and Robert O. Olsen,"A Study of the Effects of Temperature Variations on Radio Wave Absorption,"ECOM-5807, November 1976.
44. Ballard, Harold N., "Temperature Measurements in the Stratosphere from Balloon-Borne Instrument Platforms, 1968-1975," ECOM-5808, December 1976.
45. Monahan, H.H., "An Approach to the Short-Range Prediction of Early Morning Radiation Fog," ECOM-5809, January 1977.
46. Engebos, Bernard Francis, "Introduction to Multiple State Multiple Action Decision Theory and Its Relation to Mixing Structures," ECOM-5810, January 1977.
47. Low, Richard D.H.,"Effects of Cloud Particles on Remote Sensing from Space in the 10-Micrometer Infrared Region," ECOM-5811, January 1977.
48. Bonner, Robert S., and R. Newton, "Application of the AN/GVS-5 Laser Rangefinder to Cloud Base Height Measurements," ECOM-5812, February 1977.
49. Rubio, Roberto, "Lidar Detection of Subvisible Reentry Vehicle Erosive Atmospheric Material," ECOM-5813, March 1977.
50. Low, Richard D.H., and J.D. Horn, "Mesoscale Determination of Cloud-Top Height: Problems and Solutions," ECOM-5814, March 1977.

51. Duncan, Louis D., and Mary Ann Seagraves, "Evaluation of the NOAA-4 VTPR Thermal Winds for Nuclear Fallout Predictions," ECOM-5815, March 1977.
52. Randhawa, Jagir S., M. Izquierdo, Carlos McDonald and Zvi Salpeter, "Stratospheric Ozone Density as Measured by a Chemiluminescent Sensor During the Stratcom VI-A Flight," ECOM-5816, April 1977.
53. Rubio, Roberto, and Mike Izquierdo, "Measurements of Net Atmospheric Irradiance in the 0.7- to 2.8-Micrometer Infrared Region," ECOM-5817, May 1977.
54. Ballard, Harold N., Jose M. Serna, and Frank P. Hudson Consultant for Chemical Kinetics, "Calculation of Selected Atmospheric Composition Parameters for the Mid-Latitude, September Stratosphere," ECOM-5818, May 1977.
55. Mitchell, J.D., R.S. Sagar, and R.O. Olsen, "Positive Ions in the Middle Atmosphere During Sunrise Conditions," ECOM-5819, May 1977.
56. White, Kenneth O., Wendell R. Watkins, Stuart A. Schleusener, and Ronald L. Johnson, "Solid-State Laser Wavelength Identification Using a Reference Absorber," ECOM-5820, June 1977.
57. Watkins, Wendell R., and Richard G. Dixon, "Automation of Long-Path Absorption Cell Measurements," ECOM-5821, June 1977.
58. Taylor, S.E., J.M. Davis, and J.B. Mason, "Analysis of Observed Soil Skin Moisture Effects on Reflectance," ECOM-5822, June 1977.
59. Duncan, Louis D. and Mary Ann Seagraves, "Fallout Predictions Computed from Satellite Derived Winds," ECOM-5823, June 1977.
60. Snider, D.E., D.G. Murcray, F.H. Murcray, and W.J. Williams, "Investigation of High-Altitude Enhanced Infrared Backround Emissions" (U), SECRET, ECOM-5824, June 1977.
61. Dubbin, Marvin H. and Dennis Hall, "Synchronous Meteorlogical Satellite Direct Readout Ground System Digital Video Electronics," ECOM-5825, June 1977.
62. Miller, W., and B. Engebos, "A Preliminary Analysis of Two Sound Ranging Algorithms," ECOM-5826, July 1977.
63. Kennedy, Bruce W., and James K. Luers, "Ballistic Sphere Techniques for Measuring Atomspheric Parameters," ECOM-5827, July 1977.
64. Duncan, Louis D., "Zenith Angle Variation of Satellite Thermal Sounder Measurements," ECOM-5828, August 1977.
65. Hansen, Frank V., "The Critical Richardson Number," ECOM-5829, September 1977.
66. Ballard, Harold N., and Frank P. Hudson (Compilers), "Stratospheric Composition Balloon-Borne Experiment," ECOM-5830, October 1977.
67. Barr, William C., and Arnold C. Peterson, "Wind Measuring Accuracy Test of Meteorological Systems," ECOM-5831, November 1977.
68. Ethridge, G.A. and F.V. Hansen, "Atmospheric Diffusion: Similarity Theory and Empirical Derivations for Use in Boundary Layer Diffusion Problems," ECOM-5832, November 1977.
69. Low, Richard D.H., "The Internal Cloud Radiation Field and a Technique for Determining Cloud Blackness," ECOM-5833, December 1977.
70. Watkins, Wendell R., Kenneth O. White, Charles W. Bruce, Donald L. Walters, and James D. Lindberg, "Measurements Required for Prediction of High Energy Laser Transmission," ECOM-5834, December 1977.
71. Rubio, Robert, "Investigation of Abrupt Decreases in Atmospherically Backscattered Laser Energy," ECOM-5835, December 1977.
72. Monahan, H.H. and R.M. Cionco, "An Interpretative Review of Existing Capabilities for Measuring and Forecasting Selected Weather Variables (Emphasizing Remote Means)," ASL-TR-0001, January 1978.
73. Heaps, Melvin G., "The 1979 Solar Eclipse and Validation of D-Region Models," ASL-TR-0002, March 1978.

74. Jennings, S.G., and J.B. Gillespie, "M.I.E. Theory Sensitivity Studies - The Effects of Aerosol Complex Refractive Index and Size Distribution Variations on Extinction and Absorption Coefficients Part II: Analysis of the Computational Results," ASL-TR-0003, March 1978.
75. White, Kenneth O. et al, "Water Vapor Continuum Absorption in the 3.5μm to 4.0μm Region," ASL-TR-0004, March 1978.

☆ U.S. GOVERNMENT PRINTING OFFICE: 1977 777-093/ 37